

Serabelisib regulates GSDMD-mediated pyroptosis, apoptosis and migration of hepatoma cells via the PI3K/Akt/E-cadherin signaling pathway

Ming Li^{A,B,D,F}, Zhao Huang^{B,C,F}, Yuxiang Zhou^{A,B,F}

Second Department of General Surgery, Hunan Children's Hospital, Changsha, China

A – research concept and design; B – collection and/or assembly of data; C – data analysis and interpretation; D – writing the article; E – critical revision of the article; F – final approval of the article

Advances in Clinical and Experimental Medicine, ISSN 1899–5276 (print), ISSN 2451–2680 (online)

Adv Clin Exp Med. 2024;33(2):171–181

Address for correspondence

Ming Li
E-mail: liming8709@aliyun.com

Funding sources

None declared

Conflict of interest

None declared

Acknowledgements

The graphical abstract was prepared using Figdraw software.

Received on August 30, 2022

Reviewed on November 11, 2022

Accepted on May 25, 2023

Published online on July 24, 2023

Abstract

Background. Liver cancer is a malignant tumor commonly seen in infants and young children. Serabelisib is a novel and effective phosphoinositide-3-kinase (PI3K α) inhibitor, currently in trials for solid malignancy treatment, such as bladder cancer. However, it is unclear whether serabelisib affects liver cancer.

Objectives. To explore the effects of serabelisib on the proliferation, apoptosis, invasion, and metastasis of HepG2 and HuH-6 cells, and elucidate the relevant molecular mechanisms.

Materials and methods. The HepG2 cells were treated with 2 μ M, 4 μ M or 8 μ M serabelisib, while the 0- μ M group was used as a control. A plate clone formation assay was utilized to measure colony formation ability in each group, a 5-ethynyl-2'-deoxyuridine (EdU) assay examined cell proliferation, a Cell Counting Kit-8 (CCK-8) assay assessed cell viability, flow cytometry measured the cell cycle and apoptosis, JC-1 staining determined mitochondrial membrane potential, and transmission electron microscopy evaluated cell morphology. In addition, gene and protein expression levels of apoptosis markers, epithelial–mesenchymal transition (EMT), Gasdermin D (GSDMD), and the PI3K/protein kinase B (AKT) signaling pathway were measured.

Results. After serabelisib intervention, HepG2 and HuH-6 cells formed fewer colonies, proliferated more slowly, and had reduced viability. The number of HepG2 and HuH-6 cells in the G2 and S phases decreased, apoptosis and the number of apoptotic bodies increased, and mitochondrial membrane potential decreased. Serabelisib treatment also reduced the migration and invasion capacity of the cells. Furthermore, genes and proteins of the PI3K/AKT signaling pathway were downregulated, while those that promote apoptosis and pyroptosis or inhibit EMT were upregulated.

Conclusions. Serabelisib inhibited the PI3K/AKT signaling pathway, thereby inhibiting EMT and promoting apoptosis and pyroptosis in HepG2 and HuH-6 cells.

Key words: PI3K, hepatoblastoma, EMT, pyroptosis, serabelisib

Cite as

Li M, Huang Z, Zhou Y. Serabelisib regulates GSDMD-mediated pyroptosis, apoptosis and migration of hepatoma cells via the PI3K/Akt/E-cadherin signaling pathway. *Adv Clin Exp Med*. 2024;33(2):171–181. doi:10.17219/acem/166511

DOI

10.17219/acem/166511

Copyright

Copyright by Author(s)

This is an article distributed under the terms of the Creative Commons Attribution 3.0 Unported (CC BY 3.0) (<https://creativecommons.org/licenses/by/3.0/>)

Background

Liver cancer is a common malignant tumor that poses a grave threat to human life.¹ Eighty percent of liver cancers in children and adolescents are primary hepatoblastomas.² Chemotherapy and surgery are the primary treatments for hepatoblastoma,³ with cure dependent on complete excision. However, according to surgical guidelines, 60–80% of patients have nonresectable tumors at diagnosis.⁴ Therefore, researchers seek a pharmacological solution to liver cancer treatment.

Serabelisib (INK-1117, MLN-1117, TAK-117) is a novel, highly selective and effective phosphoinositide-3-kinase (PI3K α) inhibitor administered orally.⁵ The drug is currently being explored for solid malignancy treatment and has shown promising results.⁶ In addition, combining serabelisib with TAK-228 has demonstrated synergistic anti-tumor effects in preclinical bladder cancer models.⁷ Meanwhile, serabelisib pharmacokinetics continue to improve.⁸ However, the effects of serabelisib on liver cancer have not been reported.

The PI3K/protein kinase B (AKT) pathway is a classical signal transduction pathway that promotes proliferation and suppresses apoptosis. It also participates in the growth promotion and proliferation of cancer cells, promotes cellular invasion and metastasis, enhances tumor angiogenesis, and induces apoptosis resistance to chemotherapy and radiotherapy.⁹ Hartmann et al. found that the PI3K/AKT signaling pathway is usually activated in liver cancer, and in vitro PI3K targeting leads to increased apoptosis, which inhibits liver cancer cell proliferation.¹⁰ Furthermore, many substances, such as JTC-801, have been shown to inhibit HepG2 metastasis through the regulation of PI3K/AKT signaling pathway.¹¹

The PI3K/AKT signaling pathway can regulate epithelial–mesenchymal transition (EMT), a process in which epithelial cells lose their characteristics and acquire a mesenchymal phenotype under certain conditions, to reduce tumor aggression.^{12,13} It has been reported that deoxyribonucleic acid (DNA) damage-regulated autophagy modulator 1 (DRAM1) regulates liver cancer cell migration and invasion through the autophagy–EMT pathway,¹⁴ while other studies demonstrated the PI3K/AKT involvement in renal cancer cell pyroptosis.¹⁵ Pyroptosis is a form of cell death that leads to inflammation and further damage to the body.¹⁶ Several studies have found many factors related to pyroptosis, including NLRP3, interleukin (IL)-18, IL-1 β , apoptosis-associated speck-like protein containing a CARD (ASC), and caspase-1. In addition, interactions between caspase-1 and Gasdermin D (GSDMD) can lead to pyroptosis.¹⁷ Therefore, we hypothesized that serabelisib could interfere with HepG2 and HuH-6 pyroptosis through GSDMD regulation of the PI3K/Akt/E-cadherin signaling pathway.

Objectives

The study aimed to assess the effects of serabelisib on the PI3K/AKT signaling pathway in HepG2 and HuH-6 cells by exploring its impact on proliferation, apoptosis, invasion, and metastasis, and to elucidate the relevant molecular mechanisms. This research may provide a novel avenue for liver cancer treatment by establishing a new experimental and theoretical basis for the clinical study of serabelisib in liver cancer.

Materials and methods

Drug treatment

The HepG2, HuH-6, SMMC-7721, and human kidney fibroblast (HKF) cells were purchased from Abiowell (Changsha, China). The cells were digested with 0.25% trypsin solution (C0201; Beyotime Biotechnology, Shanghai, China), and cell suspensions were prepared using Roswell Park Memorial Institute (RPMI) 1640 complete medium (04-001-1ACS; Thermo Fisher Scientific, Waltham, USA). Cells were inoculated on a 6-well plate at approx. 2×10^5 cells per well and cultured overnight in a DH-160I incubator (Shanghai Sanotac Scientific Instruments Co., Ltd., Shanghai, China) at 37°C with saturated humidity and 5% carbon dioxide. The small-molecule inhibitor serabelisib (S8581; Selleckchem, Houston, USA) was dissolved in sterile dimethyl sulfoxide (DMSO) and diluted to the desired concentration. The cells in each group were treated with different drug interventions. Cells in the 0- μ M group were cultured without intervention, cells in the 2- μ M group were cultured with a medium containing 2 μ M of serabelisib, 4 μ M of serabelisib was added to the medium used to culture cells in the 4- μ M group, and the 8- μ M group had 8 μ M of serabelisib added to the medium. For the serabelisib+MK2206 group, 8 μ M of serabelisib and 3 μ M of MK2206 (IM1090; Solarbio, Beijing, China) were added to the medium. The intervention time was 48 h.

Plate clone formation assay

After 24 h of intervention, the cells were digested with a 0.25% trypsin solution and added to high-sugar Dulbecco's modified Eagle's medium (DMEM) (D5796-500mL; Thermo Fisher Scientific) to prepare cell suspensions. Then, the cells were inoculated onto a 6-well plate at a density of 1000 cells per well and shaken thoroughly.¹⁸ Afterwards, they were cultured in an incubator (37°C, 5% CO₂) for 7 days. The colony-forming ability was observed under an inverted biological microscope (model DSZ2000X; Cn-micro, Beijing, China).

5-ethynyl-2'-deoxyuridine assay

After 24 h of intervention, the 5-ethynyl-2'-deoxyuridine (EdU) DNA Proliferation in vitro Detection Kit (C10310; RiboBio, Guangzhou, China) assessed the HepG2 proliferation rate. In brief, the cells were incubated in a medium containing 50 μ M of EdU for 24 h, incubated with 1 \times Apollo[®] staining solution and then stained with 1 \times Hoechst33342 solution. Observations were made immediately after staining.

Cell Counting Kit-8 assay

The medium was aspirated, discarded and replaced with 110 μ L of Cell Counting Kit-8 (CCK-8) (NU679; Dojindo Molecular Technologies, Rockville, USA) working solution which consisted of 100 μ L of high-sugar DMEM and 10 μ L of CCK-8 stock solution. Cells were then cultured for another 4 h in a 37°C and 5% CO₂ incubator. Finally, the absorbance of each well was measured at 450 nm using a microplate analyzer (model MB-530; Shenzhen Heales Technology Development Co., Ltd., Shenzhen, China).

Flow cytometry (cell cycle)

The cells were gently suspended and separated into single cells. Then, 1.2 mL of pre-cooled 100% ethanol was added drop by drop until the concentration reached 75%. The mixed solution was stored at 4°C overnight for fixing. The next day, the cells were washed 3 times and incubated with 150 μ L of propidium iodide (PI) (MB2920; Dalian Meilunbio, Dalian, China) in the dark at 4°C for 30 min. After incubation, the cells were transferred to the flow testing tube and measured using CytoFLEX A00-1-1102 instrument (Beckman Coulter, Brea, USA).

Flow cytometry (cellular apoptosis)

An apoptosis kit (KGA108; KeyGEN Bio, Nanjing, China) was used to assess cell apoptosis. Each 2 \times 10⁵ aliquot was suspended in 500 μ L of binding buffer, and 5 μ L of annexin V-fluorescein isothiocyanate (FITC) was added to the cell suspension and mixed well. The mixture was then incubated with 5 μ L of PI in the dark at room temperature for 10 min.

JC-1 staining

A mitochondrial membrane potential assay kit with JC-1 (C2006; Beyotime Biotechnology) detected early cell apoptosis. Each 50- μ L JC-1 (200 \times) aliquot was diluted with 8 mL of ultra-pure water and mixed to obtain the JC-1 staining working solution. After incubation, the cells were washed twice with JC-1 staining buffer (1 \times) and photographed for observation.

Scratch assay

A flask of cells was digested with trypsin, counted and used to inoculate 6-well plates at 5 \times 10⁵ cells/well. When cells reached 90% confluency, they were scratched with a pipet tip, unattached cells were washed with phosphate-buffered saline (PBS), and serum-free high-sugar DMEM (D5796; Thermo Fisher Scientific) was added. The scratches were photographed and recorded at 0 h and 24 h.

Transwell migration assay

Cell suspensions were prepared using serum-free basal medium, added to the upper chambers of transwell plates (33318035; Corning Inc., Corning, USA) and incubated for 48 h. Then, the cells were immobilized for 20 min in an acetone and methanol solution (Sinopharm, Beijing, China) mixed at a 1:1 ratio. The cells were stained with 0.5% crystal violet (C8470; Solarbio) for 5 min and washed with water. Cells on the external surface were observed and imaged using an inverted microscope (model DSZ2000X; Cnmicro).

Transwell invasion assay

Sixty milliliters of Matrigel solution (356231; Corning) were diluted in 120 μ L of serum-free medium, and 60 μ L of diluted matrix glue was added to each transwell. The transwells were placed in an incubator (37°C, 60 min) to solidify the gel. Residual liquid was aspirated, 70 μ L of a basic medium was added to each transwell, and the basement membrane was hydrated at 37°C for 30 min. The cell suspension was prepared with a basic serum-free medium containing bovine serum albumin (BSA) (5 g/L), and cell density was adjusted to 1 \times 10⁵/mL. After 48 h, the Matrigel glue and cells on the upper compartment were wiped. Finally, the membranes were observed and imaged using an inverted microscope (model DSZ2000X; Cnmicro).

Immunofluorescence

Total ribonucleic acid (RNA) was extracted using TRIzol lysate (15596026; Thermo Fisher Scientific). The protocol included 0.3% Triton permeabilization for 30 min and 5% BSA blocking for 60 min at 37°C. Appropriately diluted primary antibodies, including GSDMD (20770-1-AP, 1:50; Proteintech, Rosemont, USA) and caspase-1 (22915-1-AP, 1:50; Proteintech), were added dropwise at 4°C overnight. Cells were then fixed in 4% paraformaldehyde for 10 min. Nuclei were stained with 4',6-diamidino-2-phenylindole (DAPI) working solution (AWI0331a; Abiowell) at 37°C for 10 min.

Western blot

Total cell protein was extracted using radioimmuno-precipitation (RIPA) lysate (P0013B; Beyotime Biotechnology). Separation gels with concentrations of 10%, 12% and 4.8% were prepared. After closure, membranes were incubated with primary PI3K (4249, 1:1000; Cell Signaling Technology, Danvers, USA), N-cadherin (22018-1-AP, 1:2000; Proteintech), p-AKT (4060, 1:2000; Cell Signaling Technology), E-cadherin (20874-1-AP, 1:5000; Proteintech), cytochrome C (ab184699, 1:5000; Abcam, Cambridge, UK), caspase-9 (#20750, 1:1000; Cell Signaling Technology), caspase-3 (9664, 1:1000; Cell Signaling Technology), B-cell lymphoma 2 (Bcl-2) (12789-1-AP, 1:2000; Proteintech), GSDMD (66387-1-Ig, 1:10000; Proteintech), NLRP3 (19771-1-AP, 1:800; Proteintech), caspase-1 (ab179515, 1:1000; Abcam), ASC (ab180799, 1:1000; Abcam), IL-1 β (16806-1-AP, 1:2000; Proteintech), IL-18 (ab191860, 0.25 μ g/mL; Abcam), and β -actin (66009-1-Ig, 1:5000; Proteintech) antibodies for 90 min. After incubation, the membrane was washed 3 times with PBS Triton X (PBST) solution.

Statistical analyses

All data are expressed as mean \pm standard deviation (M \pm SD). The analysis employed IBM Statistical Package for Social Sciences (SPSS) v. 26.0 software (IBM Corp., Armonk, USA). The Kolmogorov–Smirnov test analyzed data distribution, and all data displayed a normal distribution and homogeneity of variance. The data were analyzed using parametric tests, with one-way analysis of variance (ANOVA) and Tukey's post hoc test used to compare data among the 3 groups. Statistical significance was set at $p < 0.05$.

Results

Screening cell lines

First, we examined the effects of serabelisib on HepG2, HuH-6, SMMC-7721, and HKF cell proliferation. The results of the CCK-8 experiments showed that the proliferation ability of HepG2 cells in the 2- μ M, 4- μ M and 8- μ M groups significantly decreased compared to the 0- μ M group (Fig. 1A). Compared with the 0- μ M group, the proliferation ability of HuH-6 cells was significantly attenuated at 4 μ M and 8 μ M, but not at 2 μ M (Fig. 1B). The proliferation of SMMC-7721 cells was moderated at 2 μ M, 4 μ M and 8 μ M, but not to a statistically significant extent (Fig. 1C). The proliferation of HKF cells was not altered by serabelisib treatment (Fig. 1D). The raw data and analysis are presented in Supplementary Table 1. Serabelisib had no effect on normal HKF cells. Based on these findings, we selected HepG2 and HuH-6 for subsequent experiments.

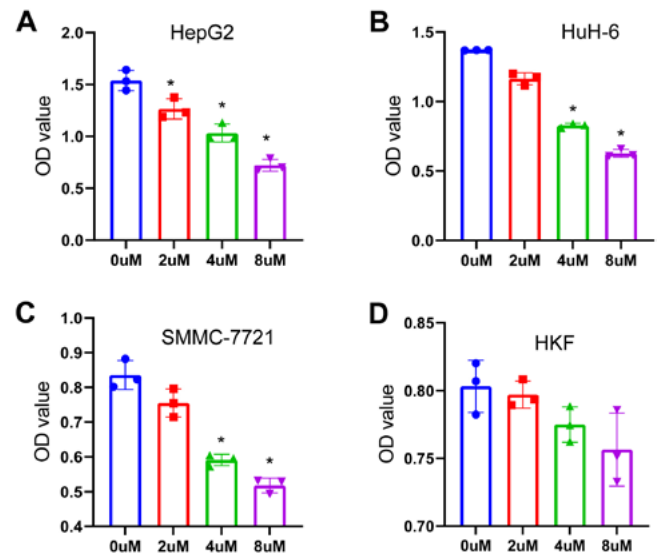


Fig. 1. Serabelisib interfered with the activity of different cells. A. The proliferation of HepG2 cells was detected with Cell Counting Kit-8 (CCK-8) assay 48 h after serabelisib treatment; B. The proliferation of HuH-6 cells was measured using CCK-8 assay 48 h after adding serabelisib; C. The proliferation of SMMC-7721 cells was measured with CCK-8 assay 48 h after adding serabelisib; D. The proliferation of human kidney fibroblasts (HKFs) was measured using CCK-8 assay 48 h after adding serabelisib. The measurement data are expressed as mean \pm standard deviation (M \pm SD). Data between multiple groups were analyzed with one-way analysis of variance (ANOVA) followed by Tukey's post hoc test ($n = 3$)

* $p < 0.05$ compared with the 0- μ M group; OD – optical density.

Serabelisib affected the PI3K/Akt/E-cadherin signaling pathway and pyroptosis

To further understand the effects of serabelisib on cells at the gene and protein levels, western blot was used to detect apoptosis and EMT-related factors in HepG2 and HuH-6 cells. Compared with the 0- μ M group, the intracellular expression levels of PI3K and p-AKT were significantly decreased in the 4- μ M and 8- μ M groups. After serabelisib intervention, the expression of Bcl-2 was decreased, while the expressions of cytochrome C, caspase-9 and caspase-3 were upregulated. Moreover, N-cadherin expression decreased, and E-cadherin expression increased in the drug intervention group, suggesting that serabelisib can affect the expression of apoptosis and EMT-related factors (Fig. 2A). We used immunofluorescence to analyze the fluorescence intensity of caspase-1 and GSDMD, and explore whether serabelisib affects pyroptosis-related factors. The results indicated that caspase-1 and GSDMD fluorescence intensity increased at 4 μ M and 8 μ M compared to the 0- μ M group (Fig. 2B). Western blot was used to detect the expression of pyroptosis-related proteins. The results showed increased pyroptosis-related expression of GSDMD, GSDMD-N, NLRP3, caspase-1, ASC, IL-1 β , and IL-18 (Fig. 2C). All data are presented in Supplementary Table 2.

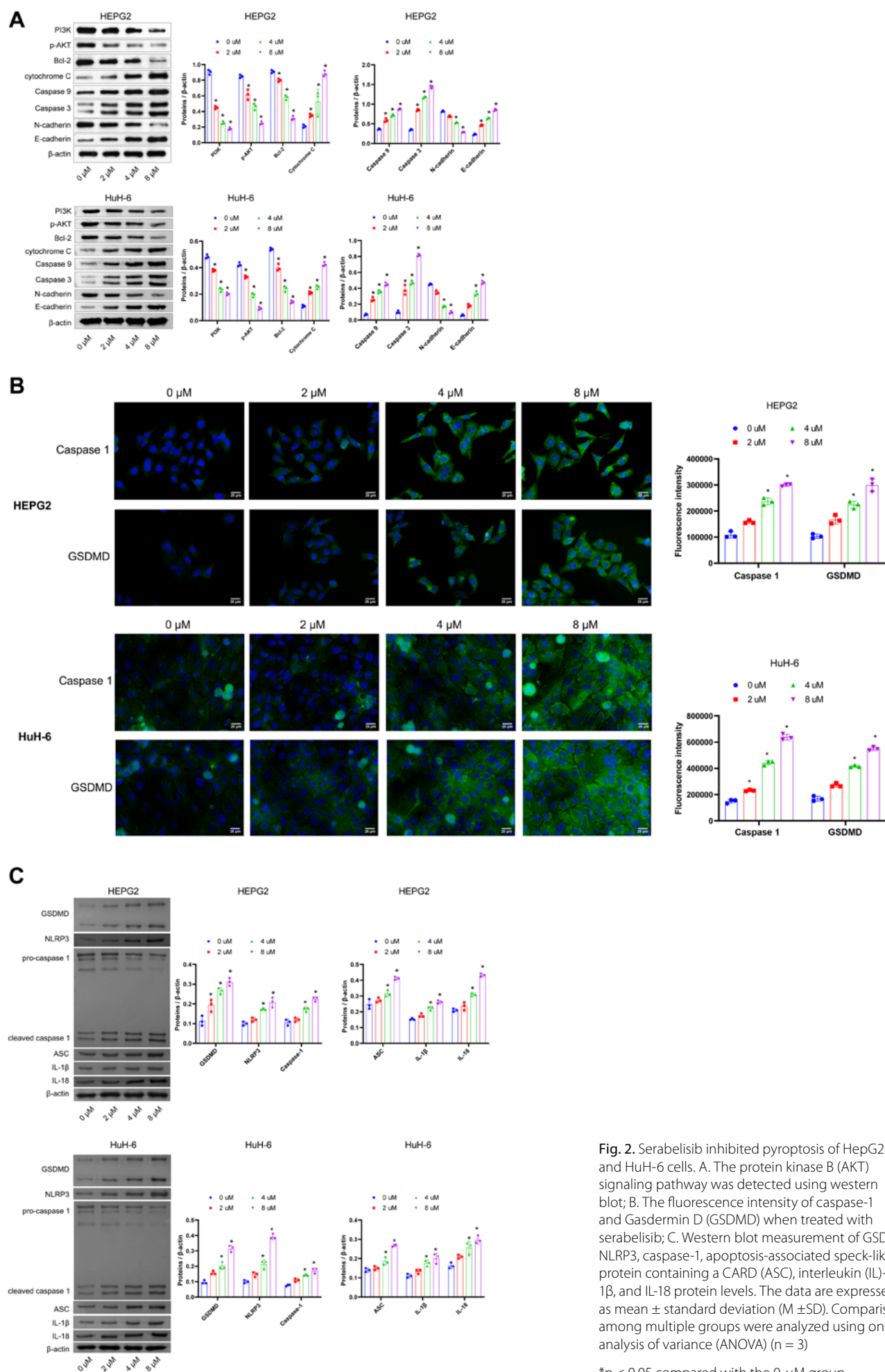


Fig. 2. Serabelisib inhibited pyroptosis of HepG2 and HuH-6 cells. A. The protein kinase B (AKT) signaling pathway was detected using western blot; B. The fluorescence intensity of caspase-1 and Gasdermin D (GSDMD) when treated with serabelisib; C. Western blot measurement of GSDMD, NLRP3, caspase-1, apoptosis-associated speck-like protein containing a CARD (ASC), interleukin (IL)-1 β , and IL-18 protein levels. The data are expressed as mean \pm standard deviation ($M \pm SD$). Comparisons among multiple groups were analyzed using one-way analysis of variance (ANOVA) ($n = 3$)

* $p < 0.05$ compared with the 0- μ M group.

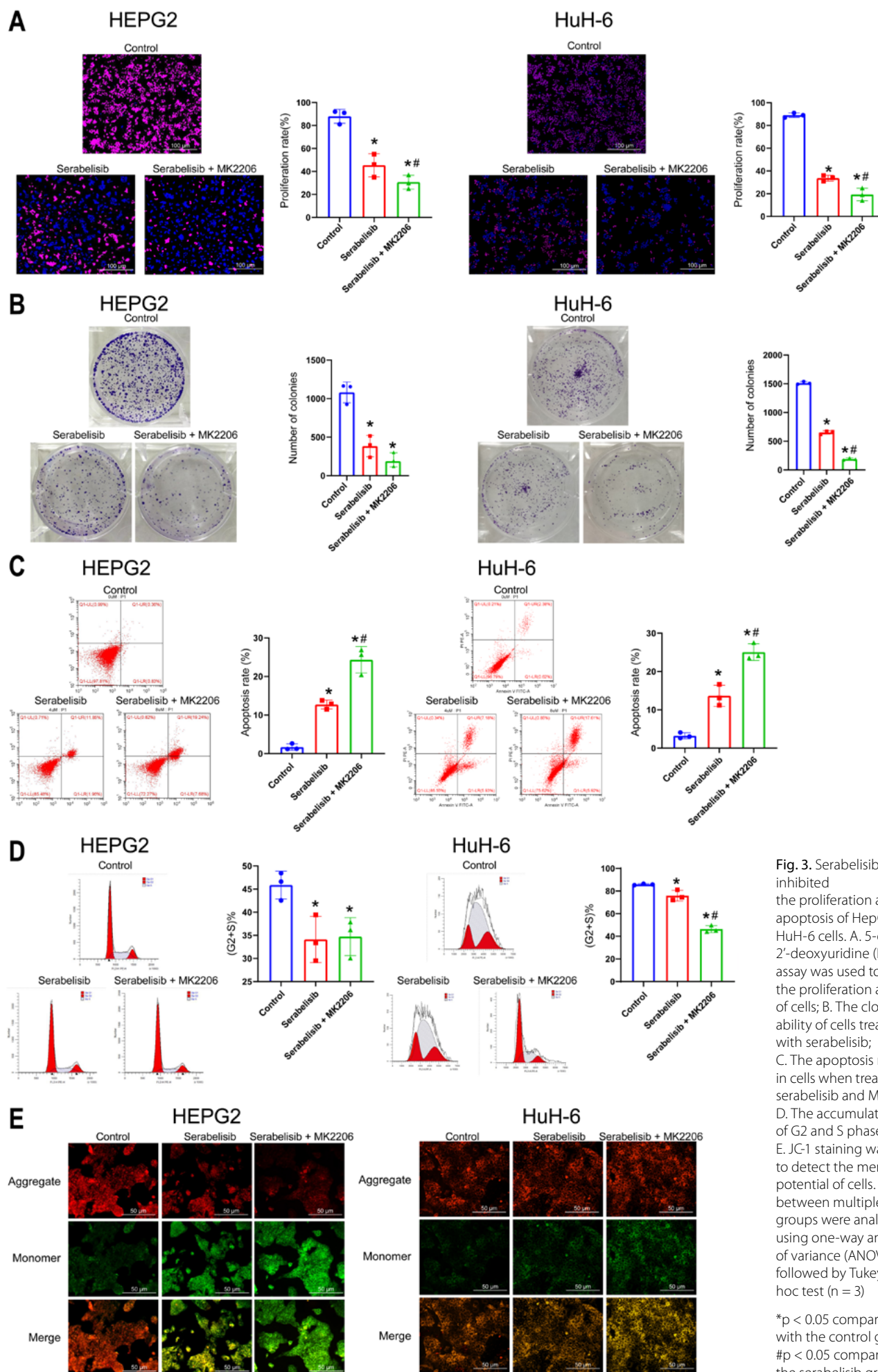


Fig. 3. Serabelisib inhibited the proliferation and apoptosis of HepG2 and HuH-6 cells. A. 5-ethynyl-2'-deoxyuridine (EdU) assay was used to assess the proliferation ability of cells; B. The cloning ability of cells treated with serabelisib; C. The apoptosis rate in cells when treated with serabelisib and MK2206; D. The accumulation of G2 and S phase cells; E. JC-1 staining was used to detect the membrane potential of cells. Data between multiple groups were analyzed using one-way analysis of variance (ANOVA) followed by Tukey's post hoc test ($n = 3$)

* $p < 0.05$ compared with the control group;
$p < 0.05$ compared with the serabelisib group.

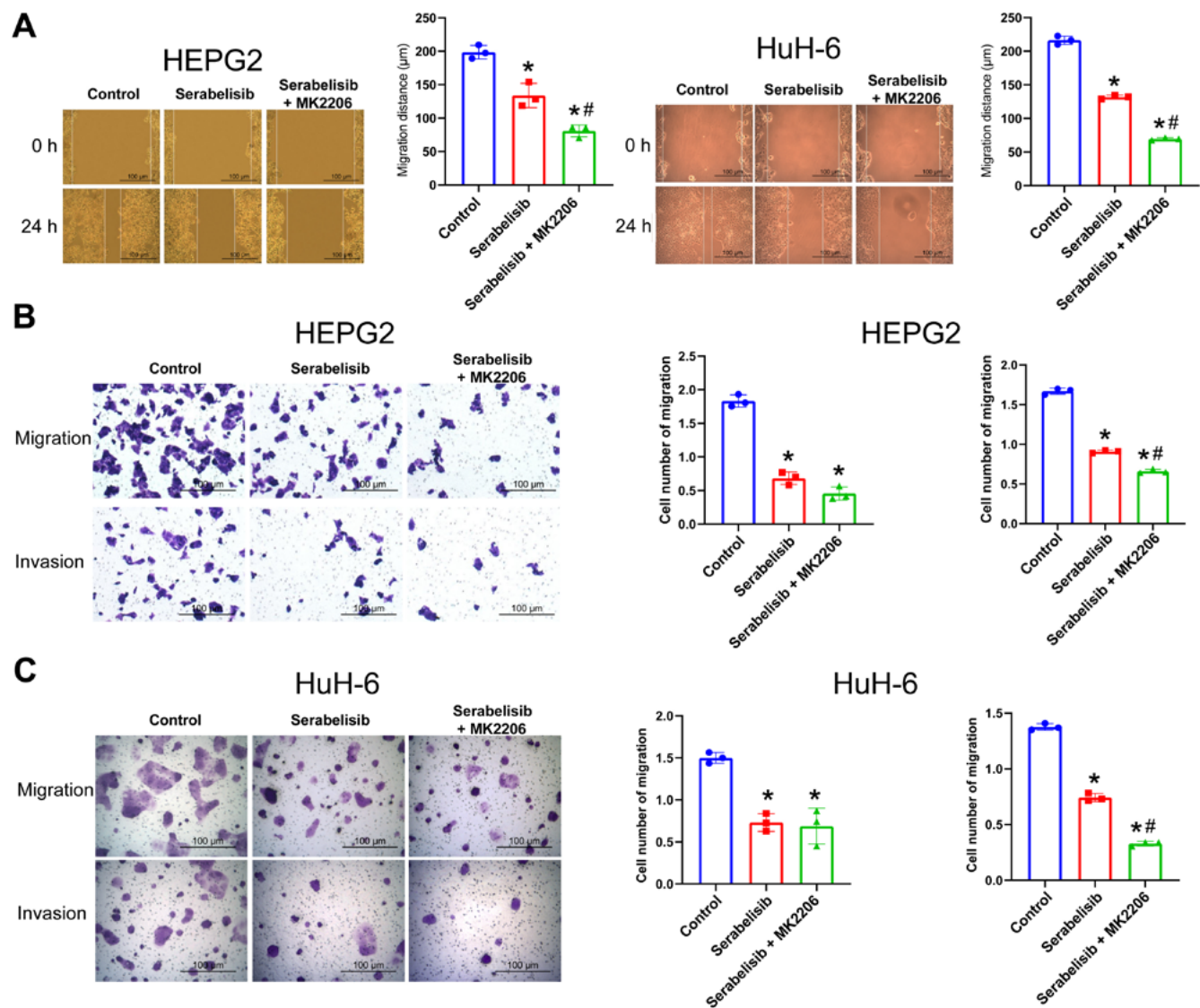


Fig. 4. Serabelisib inhibited HepG2 and HuH-6 migration and invasion. A. The migration of HepG2 and HuH-6 cells after serabelisib and MK2206 treatment; B,C. A transwell assay was used to measure the migration and invasion of HepG2 and HuH-6 cells. The measurement data are expressed as mean \pm standard deviation ($M \pm SD$). Data among multiple groups were analyzed with one-way analysis of variance (ANOVA) followed by Tukey's post hoc test ($n = 3$)

* $p < 0.05$ compared with the control group; # $p < 0.05$ compared with the serabelisib group.

In short, serabelisib affected the PI3K/Akt/E-cadherin signaling pathway and pyroptosis-related protein expression.

Serabelisib affected the proliferation and apoptosis of HepG2 and HuH-6 cells through the PI3K/Akt/E-cadherin signaling pathway

We examined the effects of serabelisib on the proliferation and apoptosis of HepG2 and HuH-6 cells. Plate clone formation and EdU experiments showed that serabelisib reduced the number of cloned colonies and weakened proliferation ability. After adding the AKT signaling pathway

inhibitor MK2206, the colony-forming ability of cells was significantly reduced (Fig. 3A,B). To investigate whether serabelisib can promote apoptosis, flow cytometry examined apoptosis and cell cycle distribution. As shown in Fig. 3C,D, the proportion of apoptotic cells increased, and the proportion of cells in the G2 and S phases decreased after the treatment with serabelisib and MK2206 in HepG2 and HuH-6 cells. Furthermore, serabelisib and MK2206 gradually increased the number of apoptotic cells, and JC-1 changed from a red polymer to a green monomer (Fig. 3E). The data and results are presented in Supplementary Table 3. Briefly, serabelisib and MK2206 can promote apoptosis and inhibit the proliferation of HepG2 and HuH-6 cells.

Serabelisib affected the migration of HepG2 and HuH-6 cells through the PI3K/Akt/E-cadherin signaling pathway

Our findings indicated that serabelisib could affect the proliferation and apoptosis of liver cancer cells through the PI3K/Akt/E-cadherin signaling pathway. The scratch method was employed to explore whether serabelisib could alter HepG2 and HuH-6 migration. Compared with the control group, the horizontal migration ability of the cells in the serabelisib group was reduced, while the horizontal migration ability was significantly reduced in the serabelisib+MK2206 group compared to the serabelisib group (Fig. 4A).

Transwell assays assessed the ability of cells to invade and migrate vertically. As shown in Fig. 4B,C, the migratory and invasive abilities of the cells in the serabelisib group were significantly reduced compared with the control group. Moreover, serabelisib+MK2206 treated cells displayed less migration and invasion capacity than the cells in the serabelisib group. The raw data and results for Fig. 4 are presented in Supplementary Table 4. In summary, serabelisib inhibited migration and invasion of HepG2 and HuH-6 cells.

Serabelisib affected GSDMD-mediated pyroptosis in HepG2 and HuH-6 cells through the PI3K/Akt/E-cadherin signaling pathway

The results indicated that serabelisib affected liver cancer cell migration and invasion. We explored whether serabelisib could affect the pyroptosis of HepG2 and HuH-6 cells using immunofluorescence to detect the pyroptosis-related caspase-1 and GSDMD. Compared with the control group, the fluorescence intensity of caspase-1 and GSDMD increased in the serabelisib group, while the fluorescence intensity increased sharply in the serabelisib+MK2206 group compared to the serabelisib group. These findings indicate that PI3K/Akt/E-cadherin signaling axis inhibition by serabelisib could increase pyroptosis-related gene expression levels (Fig. 5A).

Western blot analysis of the pyroptosis-related pathway showed increased GSDMD, NLRP3, caspase-1, ASC, IL-1 β , and IL-18 protein levels in the serabelisib group compared to the control group. Furthermore, GSDMD, NLRP3, caspase-1, ASC, IL-1 β , and IL-18 significantly increased in the serabelisib+MK2206 group compared with the serabelisib group (Fig. 5B). All raw data and analysis are presented in Supplementary Table 5. The results indicate that PI3K/Akt/E-cadherin inhibition using serabelisib can promote pyroptosis-related gene expression in cells and trigger pyroptosis.

Discussion

Liver cancer originates from abnormal stem cells and hepatic epithelial progenitor cells,¹⁹ and is a malignant embryonic liver tumor commonly found in infants and young children, accounting for around 80% of pediatric liver cancer cases.¹⁹ Currently, liver cancer therapy includes adjuvant chemotherapy, hepatectomy and liver transplantation. Unfortunately, the survival rate is only 60% for high-risk patients.²⁰ Serabelisib is an effective oral selective PI3K α inhibitor currently being explored for clinical use in cancer treatment.²¹ In this study, serabelisib was tested in vitro to assess a range of cell functions. We found that serabelisib promoted apoptosis in a dose-dependent manner. To further explain its mechanism of action, we examined the cellular gene and protein levels.

The PI3K/AKT axis contributes to oncogenic transformation, and its possible mechanisms include stimulation of proliferation, metastasis, and the inhibition of autophagy and senescence.²² Apoptosis is a form of programmed cell death regulated by proteins of the Bcl-2 and caspase families,²³ with *Bcl-2* being an anti-apoptotic gene and an important target for cancer therapy.²⁴ The best biochemical marker recognized for early and late apoptosis detection is cysteine protease activation.²⁵ During apoptosis, caspase-3 acts as an executor and has an important proteolytic function, regulating the final stage of programmed cell death.²⁶ According to reports, lncRNA prostate cancer-associated transcript 1 (PCAT1) interacts with dyskerin pseudouridine synthase 1 to regulate proliferation, invasion and apoptosis in non-small cell lung cancer cells via the vascular endothelial growth factor (VEGF)/AKT/Bcl-2/caspase-9 pathway.²⁷ We found that serabelisib inhibited expression of PI3K, AKT and Bcl-2 in cells, while the expression of cytochrome C, caspase-9 and caspase-3 was elevated. In summary, serabelisib promotes HepG2 and HuH-6 apoptosis by inhibiting the PI3K/AKT signaling pathway.

Tumor metastasis and recurrence are key barriers to a complete liver cancer cure.²⁸ Epithelial–mesenchymal transition is necessary for promoting migration and invasion of tumor cells, and is often characterized by decreased epithelial E-cadherin and increased N-cadherin.^{29,30} The EMT of hepatocellular carcinoma (HCC) is considered crucial in intrahepatic dissemination and distal metastasis.³¹ During EMT, epithelial cells lose their polygonal shape and acquire a fusiform conformation, resulting in enhanced tumor cell motility and invasion abilities.³² In HCC, the protein arginine methyltransferase activates EMT by regulating the PI3K/AKT signaling pathway to promote HCC cell invasion and lung metastasis.³³ In this study, the results indicate that PI3K, p-AKT and E-cadherin expression levels in HepG2 and HuH-6 cells decreased after serabelisib intervention, while the expression of N-cadherin increased, and the effect was dose-dependent.

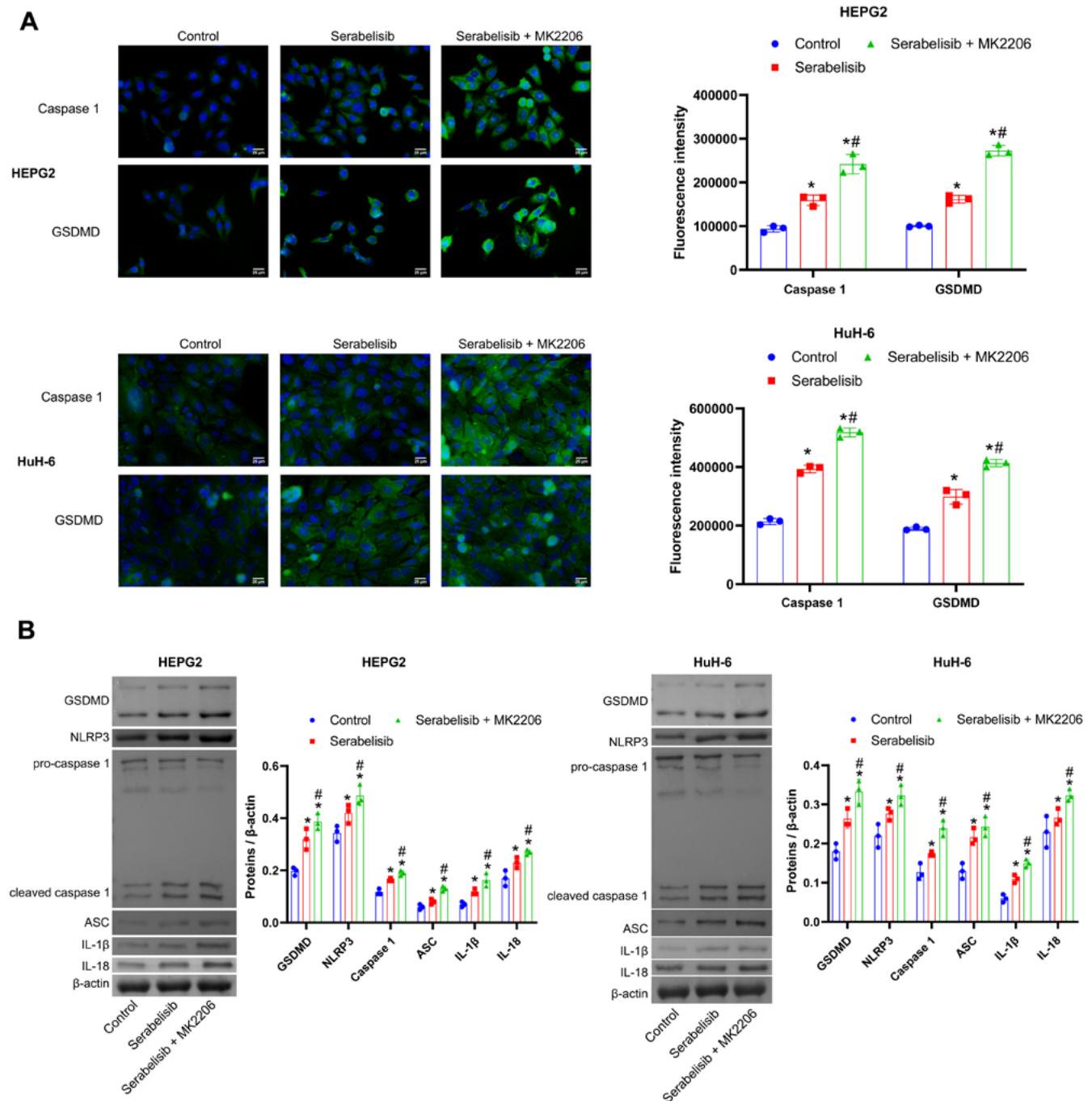


Fig. 5. Serabelisib promoted pyroptosis in HepG2 and HuH-6 cells. A. The fluorescence intensity of caspase-1 and Gasdermin D (GSDMD) was measured with immunofluorescence; B. The expression levels of pyroptosis-related genes. The data are expressed as mean \pm standard deviation ($M \pm SD$). Comparisons among multiple groups were analyzed using a one-way analysis of variance (ANOVA) ($n = 3$)

* $p < 0.05$ compared with the control group; # $p < 0.05$ compared with the serabelisib group; ASC – apoptosis-associated speck-like protein containing a CARD; IL – interleukin.

Limitations

Our future research will focus on investigating the effects of serabelisib on tissue growth in xeno-transplantation tumor models. The current study demonstrated that serabelisib inhibited liver cancer development in a dose-dependent manner and explained its

molecular mechanisms, providing a theoretical basis for its formal application in the clinical treatment of liver cancer. However, this study only involved mouse models and did not include a wider population or clinical trials. Therefore, further research is needed to determine the potential and efficacy of serabelisib in treating liver cancer.

Conclusions

Serabelisib inhibited cell migration and invasion by blocking EMT through the PI3K/AKT signaling pathway. Remarkably, GSDMD, a major pyroptosis effector, was repressed by serabelisib. We believe that pyroptosis plays a vital role in liver cancer and is inhibited by serabelisib. Serabelisib inhibited apoptosis and pyroptosis at the gene and protein levels.

Supplementary data

The supplementary materials are available at <https://doi.org/10.5281/zenodo.7964600>. The package contains the following files:

Supplementary Table 1. Proliferation ability of HepG2, HuH-6, SMMC-7721, and HKF cells in the 2- μ M, 4- μ M and 8- μ M groups (for Fig. 1).

Supplementary Table 2. Expression of PI3K/Akt/E-cadherin signaling pathway and pyroptosis (for Fig. 2).


Supplementary Table 3. Proliferation and apoptosis of HepG2 and HuH-6 cells (for Fig. 3).


Supplementary Table 4. Migration of HepG2 and HuH-6 cells through the PI3K/Akt/E-cadherin signaling pathway (for Fig. 4).

Supplementary Table 5. Pyroptosis of GSDMD-mediated HepG2 and HuH-6 cells through the PI3K/Akt/E-cadherin signaling pathway (for Fig. 5).

ORCID iDs

Ming Li  <https://orcid.org/0009-0009-8169-6591>

Zhao Huang  <https://orcid.org/0009-0001-1934-2831>

Yuxiang Zhou  <https://orcid.org/0009-0004-7357-4192>

References

- Lim I, Bondoc A, Geller J, Tiao G. Hepatoblastoma: The evolution of biology, surgery, and transplantation. *Children (Basel)*. 2018;6(1):1. doi:10.3390/children6010001
- Ranganathan S, Lopez-Terrada D, Alaggio R. Hepatoblastoma and pediatric hepatocellular carcinoma: An update. *Pediatr Dev Pathol*. 2020;23(2):79–95. doi:10.1177/1093526619875228
- Yang T, Whitlock RS, Vasudevan SA. Surgical management of hepatoblastoma and recent advances. *Cancers (Basel)*. 2019;11(12):1944. doi:10.3390/cancers11121944
- Trobaugh-Lotrario AD, Meyers RL, O'Neill AF, Feusner JH. Unresectable hepatoblastoma: Current perspectives. *Hepat Med*. 2017;9:1–6. doi:10.2147/HMER.S89997
- Juric D, De Bono JS, LoRusso PM, et al. A first-in-human, phase I, dose-escalation study of TAK-117, a selective PI3K α isoform inhibitor, in patients with advanced solid malignancies. *Clin Cancer Res*. 2017;23(17):5015–5023. doi:10.1158/1078-0432.CCR-16-2888
- Bottino DC, Patel M, Kadakia E, et al. Dose optimization for anticancer drug combinations: Maximizing therapeutic index via clinical exposure-toxicity/preclinical exposure-efficacy modeling. *Clin Cancer Res*. 2019;25(22):6633–6643. doi:10.1158/1078-0432.CCR-18-3882
- Hernández-Prat A, Rodríguez-Vida A, Juanpere-Rodero N, et al. Novel oral mTORC1/2 inhibitor TAK-228 has synergistic antitumor effects when combined with paclitaxel or PI3K α inhibitor TAK-117 in pre-clinical bladder cancer models. *Mol Cancer Res*. 2019;17(9):1931–1944. doi:10.1158/1541-7786.MCR-18-0923
- Patel CG, Rangachari L, Patti M, Griffin C, Shou Y, Venkatakrishnan K. Characterizing the sources of pharmacokinetic variability for TAK-117 (Serabelisib), an investigational phosphoinositide 3-kinase α inhibitor: A clinical biopharmaceutics study to inform development strategy. *Clin Pharmacol Drug Dev*. 2019;8(5):637–646. doi:10.1002/cpdd.613
- Cui X, Liu X, Han Q, et al. DPEP1 is a direct target of miR-193a-5p and promotes hepatoblastoma progression by PI3K/Akt/mTOR pathway. *Cell Death Dis*. 2019;10(10):701. doi:10.1038/s41419-019-1943-0
- Hartmann W, Küchler J, Koch A, et al. Activation of phosphatidylinositol 3'-kinase/AKT signaling is essential in hepatoblastoma survival. *Clin Cancer Res*. 2009;15(14):4538–4545. doi:10.1158/1078-0432.CCR-08-2878
- Zhao B, Hu T. JTC-801 inhibits the proliferation and metastasis of the Hep G2 hepatoblastoma cell line by regulating the phosphatidylinositol 3-kinase/protein kinase B signalling pathway. *Oncol Lett*. 2018;17(2):1939–1945. doi:10.3892/ol.2018.9780
- Xu W, Yang Z, Lu N. A new role for the PI3K/Akt signaling pathway in the epithelial-mesenchymal transition. *Cell Adh Migr*. 2015;9(4):317–324. doi:10.1080/19336918.2015.1016686
- Georgakopoulos-Soares I, Chartoumpakis DV, Kyriazopoulou V, Zaravinos A. EMT factors and metabolic pathways in cancer. *Front Oncol*. 2020;10:499. doi:10.3389/fonc.2020.00499
- Chen C, Liang Q, Chen H, et al. DRAM1 regulates the migration and invasion of hepatoblastoma cells via autophagy-EMT pathway. *Oncol Lett*. 2018;16(2):2427–2433. doi:10.3892/ol.2018.8937
- Zhang C, Lin T, Nie G, et al. Cadmium and molybdenum co-induce pyroptosis via ROS/PTEN/PI3K/AKT axis in duck renal tubular epithelial cells. *Environ Pollut*. 2021;272:116403. doi:10.1016/j.envpol.2020.116403
- Jia Y, Cui R, Wang C, et al. Metformin protects against intestinal ischemia-reperfusion injury and cell pyroptosis via TXNIP-NLRP3-GSDMD pathway. *Redox Biol*. 2020;32:101534. doi:10.1016/j.redox.2020.101534
- Xu S, Wang J, Zhong J, et al. CD73 alleviates GSDMD-mediated microglia pyroptosis in spinal cord injury through PI3K/AKT/Foxo1 signaling. *Clin Transl Med*. 2021;11(1):e269. doi:10.1002/ctm2.269
- Liu L, Wang J, Sun G, et al. m6A mRNA methylation regulates CTNNB1 to promote the proliferation of hepatoblastoma. *Mol Cancer*. 2019;18(1):188. doi:10.1186/s12943-019-1119-7
- Allan BJ, Parikh PP, Diaz S, Perez EA, Neville HL, Sola JE. Predictors of survival and incidence of hepatoblastoma in the paediatric population. *HPB (Oxford)*. 2013;15(10):741–746. doi:10.1111/hpb.12112
- Zhen N, Gu S, Ma J, et al. CircHMGCS1 promotes hepatoblastoma cell proliferation by regulating the IGF signaling pathway and glutaminolysis. *Theranostics*. 2019;9(3):900–919. doi:10.7150/thno.29515
- Jessen KA, Kessler L, Kucharski J, et al. Abstract 4501: INK117: A potent and orally efficacious PI3K α -selective inhibitor for the treatment of cancer. *Cancer Res*. 2011;71(8 Suppl):4501–4501. doi:10.1158/1538-7445.AM2011-4501
- Aoki M, Fujishita T. Oncogenic roles of the PI3K/AKT/mTOR axis. In: Hunter E, Bister K, eds. *Viruses, Genes, and Cancer*. Current Topics in Microbiology and Immunology. Vol. 407. Cham, Switzerland: Springer International Publishing; 2017:153–189. doi:10.1007/82_2017_6
- Brentnall M, Rodriguez-Menocal L, De Guevara RL, Cepero E, Boise LH. Caspase-9, caspase-3 and caspase-7 have distinct roles during intrinsic apoptosis. *BMC Cell Biol*. 2013;14(1):32. doi:10.1186/1471-2121-14-32
- Ebrahim AS, Sabbagh H, Liddane A, Raufi A, Kandouz M, Al-Katib A. Hematologic malignancies: Newer strategies to counter the BCL-2 protein. *J Cancer Res Clin Oncol*. 2016;142(9):2013–2022. doi:10.1007/s00432-016-2144-1
- Mazumder S, Plesca D, Almasan A. Caspase-3 activation is a critical determinant of genotoxic stress-induced apoptosis. In: Mor G, Alvero AB, eds. *Apoptosis and Cancer*. Totowa, USA: Humana Press; 2008:13–21. doi:10.1007/978-1-59745-339-4_2
- Nichani K, Li J, Suzuki M, Houston JP. Evaluation of caspase-3 activity during apoptosis with fluorescence lifetime-based cytometry measurements and phasor analyses. *Cytometry*. 2020;97(12):1265–1275. doi:10.1002/cyto.a.24207
- Liu SY, Zhao ZY, Qiao Z, Li SM, Zhang WN. LncRNA PCAT1 interacts with DKC1 to regulate proliferation, invasion and apoptosis in NSCLC cells via the VEGF/AKT/Bcl2/caspase-9 pathway. *Cell Transplant*. 2021;30:096368972098607. doi:10.1177/0963689720986071

28. Lu C, Xiangdong T, Wenchen G, et al. Periostin mediates epithelial–mesenchymal transition through the MAPK/ERK pathway in hepatoblastoma. *Cancer Biol Med*. 2019;16(1):89. doi:10.20892/j.issn.2095-3941.2018.0077
29. Fu X, Cui P, Chen F, et al. Thymosin β 4 promotes hepatoblastoma metastasis via the induction of epithelial–mesenchymal transition. *Mol Med Rep*. 2015;12(1):127–132. doi:10.3892/mmr.2015.3359
30. Xie X, Zhu H, Zhang J, et al. Solamargine inhibits the migration and invasion of HepG2 cells by blocking epithelial-to-mesenchymal transition. *Oncol Lett*. 2017;14(1):447–452. doi:10.3892/ol.2017.6147
31. Zucchini-Pascal N, Peyre L, Rahmani R. Crosstalk between beta-catenin and Snail in the induction of epithelial to mesenchymal transition in hepatocarcinoma: Role of the ERK1/2 pathway. *Int J Mol Sci*. 2013;14(10):20768–20792. doi:10.3390/ijms141020768
32. Pastushenko I, Blanpain C. EMT transition states during tumor progression and metastasis. *Trends Cell Biol*. 2019;29(3):212–226. doi:10.1016/j.tcb.2018.12.001
33. Jiang H, Zhou Z, Jin S, et al. PRMT 9 promotes hepatocellular carcinoma invasion and metastasis via activating PI 3K/Akt/GSK-3 β /Snail signaling. *Cancer Sci*. 2018;109(5):1414–1427. doi:10.1111/cas.13598